"Supporting Information"

Mechanistic Insights into the Regio- and Stereoselectivity of [3+2] Cycloaddition Reactions between N-methyl-phenylnitrone and trans-1-chloro-2-nitroethylene within the Framework of Molecular Electron Density Theory

Sofiane Benmetir[ab], Mohamed Chellegui[*cd], Lakhdar Benhamed[e], Raghad Mowafak Al-Mokhtar[f], Raad Nasrullah Salih[g], Muheb Amjad Algso[h], Jesus Vicente de Julián-Ortiz[a] and Haydar A. Mohammad-Salim[ij]

[a] *Department of Physical Chemistry, Faculty of Pharmacy, University of Valencia, Av. Vicente Andrés Estellés s/n, 46100 Valencia, Spain*

[b] *Process and Environmental Engineering Laboratory (LIPE), Faculty of Chemistry, University of Science and Technology of Oran Mohamed BOUDIAF, P.O. Box 1503, El Mnaouer, 31000 Oran, Algeria*

[c] *Laboratory of Organic Chemistry (LR17ES08), Faculty of Sciences, University of Sfax, 3038 Sfax, Tunisia*

[d] *Namur Institute of Structured Matter, University of Namur, Rue de Bruxelles, 61, B-5000 Namur, Belgium*

[e] *Laboratory of Applied Thermodynamics and Molecular Modelling, Department of Chemistry, Faculty of Sciences, Abou-Bekr Belkaid University, PO 119, Tlemcen, 13000, Algeria.*

[f] *Department of Chemistry, College of Science, University of Duhok, Duhok 42001, Kurdistan Region, Iraq*

[g] *Nursing Department, Bardarash Technical Institute, Akre University for Applied science, Duhok 42001, Kurdistan Region, Iraq*

[h] *Department of Chemistry, College of Science, University of Duhok, Duhok 42001, Kurdistan Region, Iraq*

[i] *Department of Chemistry, Faculty of Science, University of Zakho, Zakho 42002, Kurdistan Region, Iraq*

[j] *TCCG Lab, Scientific Research Center, University of Zakho, Zakho 42002, Kurdistan Region, Iraq*

In this study, the 32CA reactions between both the Z- and E-isomers of N-methyl-phenylnitrone **1** and trans-1-chloro-2-nitroethylene **2** were investigated using density functional theory (DFT) calculations at the IEFPCM(benzene)/B3LYP/6-311G(d,p) level of theory. The reaction involving the Z-isomer of nitrone **1** is illustrated in **Scheme S1**, while that with the E-isomer is shown in **Scheme S2**.

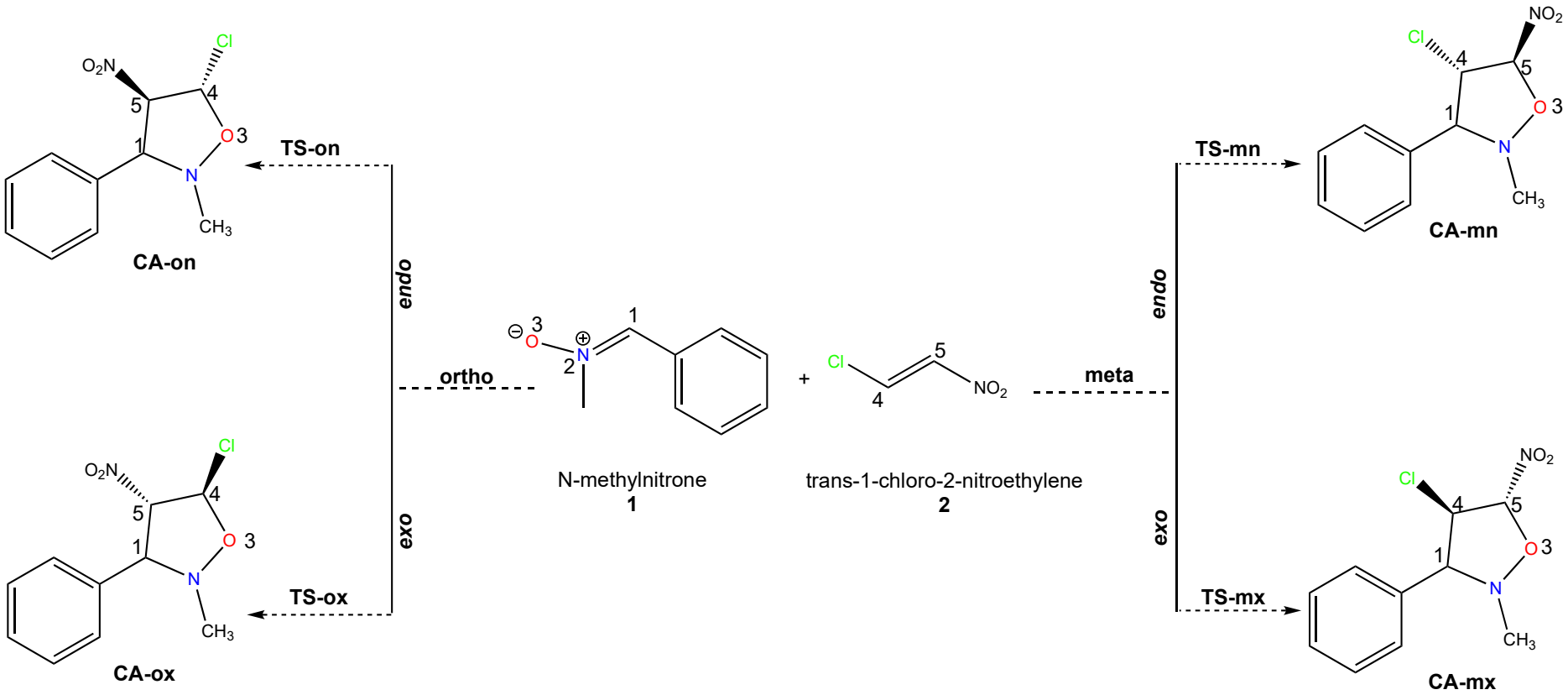

Scheme S1. Possible regio- and stereoisomeric pathways for the 32CA reaction between Z-isomer of N-methyl-phenylnitrone **1** and trans-1-chloro-2-nitroethylene **2** leading to the formation of cycloadducts.

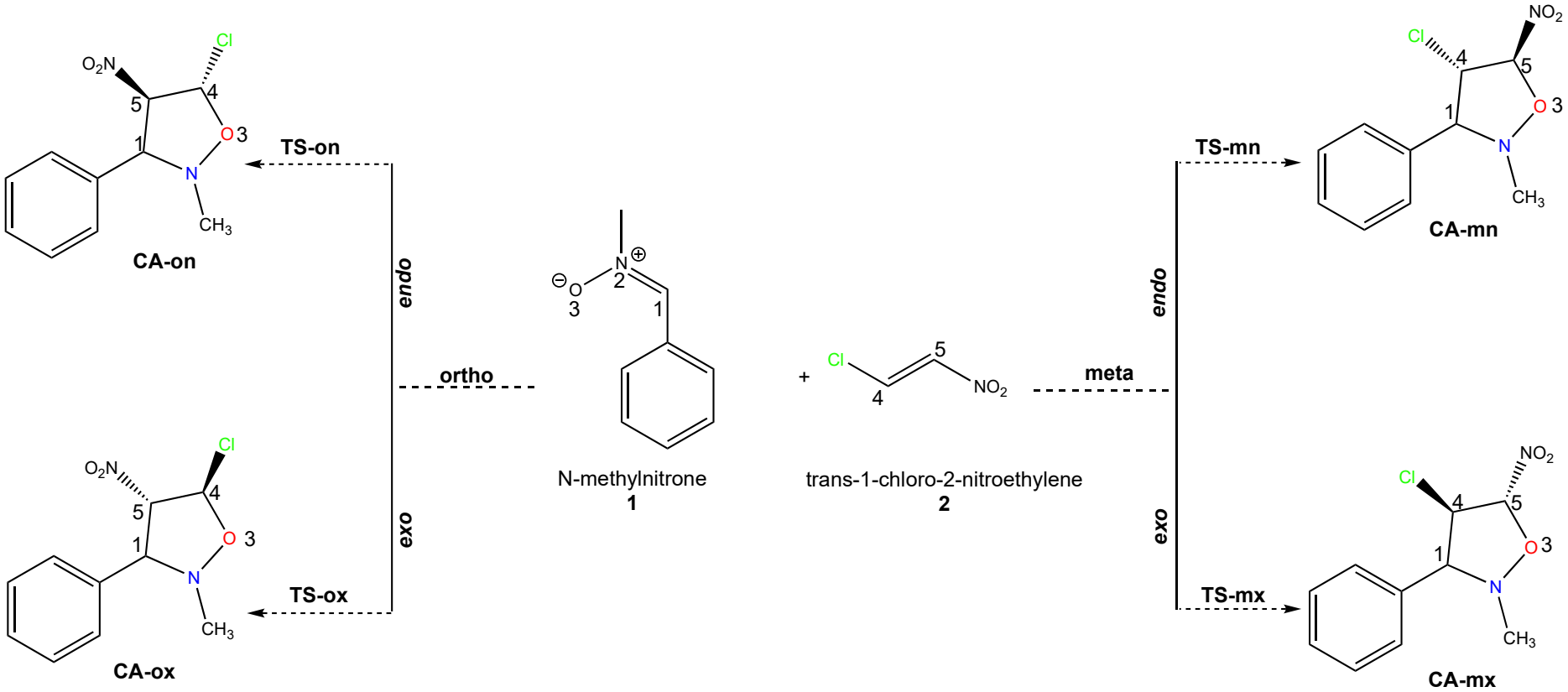

Scheme S2. Possible regio- and stereoisomeric pathways for the 32CA reaction between E-isomer of N-methyl-phenylnitrone **1** and trans-1-chloro-2-nitroethylene **2** leading to the formation of cycloadducts.

The relative values of energy (E), enthalpy (H^0), entropy (S^0) and Gibbs enthalpy (G^0) of the reactants, products, and calculated at different levels of theory are given in Table S1.

Table S1 Energies, enthalpies, entropies, and Gibbs enthalpies of reactants, transition states, and products calculated at different levels of theory. Solvent (benzene) effects were described using IEFPCM.

Systems	E (a.u.)	H° (a.u.)	S^0 (cal mol^{-1} K^{-1})	G° (a.u.)
B3LYP/6-311G(d,p)				
1-Z	-440.287244	-440.123006	92.126	-440.166778
2	-742.790695	-742.738231	78.183	-742.775378
CA-on	-1183.110444	-1182.889267	121.399	-1182.946948
CA-ox	-1183.11389172	-1182.893149	122.663	-1182.951430
CA-mn	-1183.102561	-1182.881634	121.670	-1182.939443
CA-mx	-1183.10719523	-1182.886132	123.695	-1182.944904
TS-on	-1183.066935	-1182.848840	125.260	-1182.908355
TS-ox	-1183.06950818	-1182.851448	121.489	-1182.904770
TS-mn	-1183.059235	-1182.841145	122.124	-1182.909171
TS-mx	-1183.05924027	-1182.841320	124.315	-1182.900386
B3LYP/6-311G(d,p)				
1-E	-440.298019	-440.133627	91.956	-440.177318
CA-on	-1183.110392	-1182.889594	122.025	-1182.947572
CA-ox	-1183.117759	-1182.896816	123.888	-1182.955680
CA-mn	-1183.116661	-1182.895738	122.793	-1182.954081
CA-mx	-1183.107195	-1182.886132	123.695	-1182.944904
TS-on	-1183.063701	-1182.846111	123.397	-1182.904741
TS-ox	-1183.069508	-1182.851441	121.407	-1182.909126
TS-mn	-1183.057213	-1182.839547	123.602	-1182.898274
TS-mx	-1183.054652	-1182.836989	124.265	-1182.896032
M062X/6-311G(d,p)				
1-Z	-440.088443	-439.922363	91.144	-439.965668
2	-742.642536	-742.589050	77.926	-742.626075
CA-on	-1182.794974	-1182.570612	118.806	-1182.627060

CA-ox	-1182.797514	-1182.573649	121.103	-1182.631189
CA-mn	-1182.787193	-1182.562852	119.326	-1182.619548
CA-mx	-1182.794078	-1182.569802	119.540	-1182.626599
TS-on	-1182.734593	-1182.513680	124.406	-1182.572789
TS-ox	-1182.741683	-1182.520929	120.939	-1182.578391
TS-mn	-1182.728177	-1182.506944	120.117	-1182.564016
TS-mx	-1182.736220	-1182.515921	121.064	-1182.573442
		ωB97X-D/6-311G(d,p)		
1-Z	-440.127914	-439.961968	91.383	-440.005387
2	-742.673370	-742.620126	78.059	-742.657214
CA-on	-1182.860341	-1182.636231	119.757	-1182.693131
CA-ox	-1182.862343	-1182.638631	120.618	-1182.695941
CA-mn	-1182.851701	-1182.627905	120.369	-1182.685096
CA-mx	-1182.858389	-1182.634412	120.287	-1182.691565
TS-on	-1182.800712	-1182.579850	123.880	-1182.638710
TS-ox	-1182.806163	-1182.585452	120.391	-1182.642654
TS-mn	-1182.795018	-1182.574157	120.514	-1182.631417
TS-mx	-1182.795013	-1182.574327	122.787	-1182.632667

Table S2 Relative energies (ΔE) and Gibbs free energies (ΔG), in kcal mol^{-1}, for TSs and cycloadducts involved in the 32CA between N-methyl-phenylnitrone **1** and trans-1-chloro-2-nitroethylene **2**, in benzene at room temperature calculated at different levels of theory. The electronic and steric contributions, ΔH and –TΔS, respectively, are included.

	ΔE	**ΔH**	**-TΔS**	**ΔG**
		M06-2X/6-311G(d,p)		

TS-on	-6.72	-5.97	14.35	8.38
TS-ox	-2.27	-1.42	13.32	11.89
TS-mn	1.76	2.80	14.59	17.40
TS-mx	1.76	2.80	14.59	17.40
CA-on	-41.75	-39.05	14.30	-24.75
CA-ox	-40.16	-37.15	14.99	-22.16
CA-mn	-35.27	-32.28	14.83	-17.45
CA-mx	-35.27	-32.28	14.83	-17.45
		ωB97X-D/6-311G(d,p)		
TS-on	-3.06	-2.11	0.00	12.52
TS-ox	0.36	1.41	-1.04	14.99
TS-mn	3.93	4.98	14.59	19.57
TS-mx	3.93	4.98	-0.04	19.57
CA-on	-38.32	-35.48	0.00	-20.92
CA-ox	-37.06	-33.97	0.26	-19.16
CA-mn	-31.64	-28.75	14.63	-14.12
CA-mx	-31.64	-28.75	0.07	-14.12

Table S3 B3LYP/6-311G(d,p) relative energy, entahlpy and Gibbs free energy (kcal mol^{-1}) of Z-isomer comparing to E-isomer of N-methyl-phenylnitrone **1** in benzene at room temperature.

Isomer	**ΔE**	**ΔH**	**ΔG**
E	0.00	0.00	0.00
Z	6.76	6.66	6.61

Table S4 B3LYP/6-311G(d,p) relative energies (ΔE, in kcal mol^{-1}), enthalpies (ΔH, in kcal mol^{-1}), entropies (ΔS, in $calmol^{-1}$ K^{-1}) and Gibbs free energies (ΔG, in kcal mol^{-1}), for TSs and cycloadducts involved in the 32CA between E-N-methyl-phenylnitrone **1** and trans-1-chloro-2-nitroethylene **2**, in benzene.

	ΔE	**ΔH**	**TΔS(-)**	**ΔG**
TS-ox	15.70	16.16	13.94	30.09
TS-on	14.66	15.27	13.89	29.16
TS-mx	19.77	20.28	13.87	34.15
TS-mn	21.37	21.88	13.68	35.56
CA-ox	-13.63	-10.92	14.53	3.61
CA-on	-15.80	-13.36	14.15	0.79
CA-mx	-8.69	-6.13	14.45	8.32
CA-mn	-11.60	-8.96	13.85	4.89

Table S5 B3LYP/6-311G(d,p) Maxwell−Boltzmann weight (P in %) for the all the studied cycloadducts involved in the 32CA reaction between Z-N-methyl-phenylnitrone **1** and trans-1-chloro-2-nitroethylene **2**, in benzene.

Structures	**CA-on**	**CA-ox**	**CA-mn**	**CA-mx**
P	99.40	0.58	0.02	0.00

Table S6 B3LYP/6-311G(d,p) electronic and steric contributions (in %), ΔH and -T ΔS, to relative relative Gibbs free energies, in kcal/mol, for TSs involved in the 32CA of E-isomer and Z-isomer of N-methyl-phenylnitrone **1** with trans-1-chloro-2-nitroethylene **2**, in benzene.

	ΔH	**-TΔS**	**ΔG**
		Z-isomer	
TS-ox	7.78(29.7%)	13.43(70.3%)	21.21
TS-on	6.14(36.7%)	14.56(63.3%)	20.70
TS-mx	12.61(47.7%)	14.37(52.3%)	26.97

TS-mn	12.50(46.8%)	13.71(53.2%)	26.21
		E-isomer	
TS-ox	16.16(53.7%)	13.94(46.3%)	30.09
TS-on	15.27(52.3%)	13.89(47.6%)	29.16
TS-mx	20.28(59.4%)	13.87(40.6%)	34.15
TS-mn	21.88(61.5%)	13.68(38.5%)	35.56

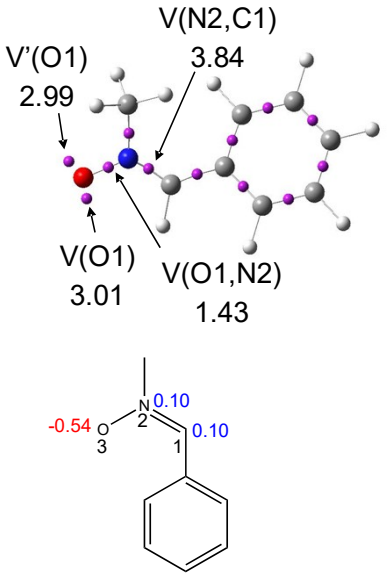

Fig. S1 B3LYP/6–311G(d,p) calculated ELF localization domains (isosurface value of ELF = 0.80), and proposed Lewis-like structures, together with the natural atomic charges, in average number of electrons e, E-isomers of N-methyl-phenylnitrone **1** in benzene at room temperature. Protonated basins are shown in blue, monosynaptic basins in red, disynaptic basins in green, and core basins in magenta colours. Negative charges are coloured in red, and positive charges in blue.

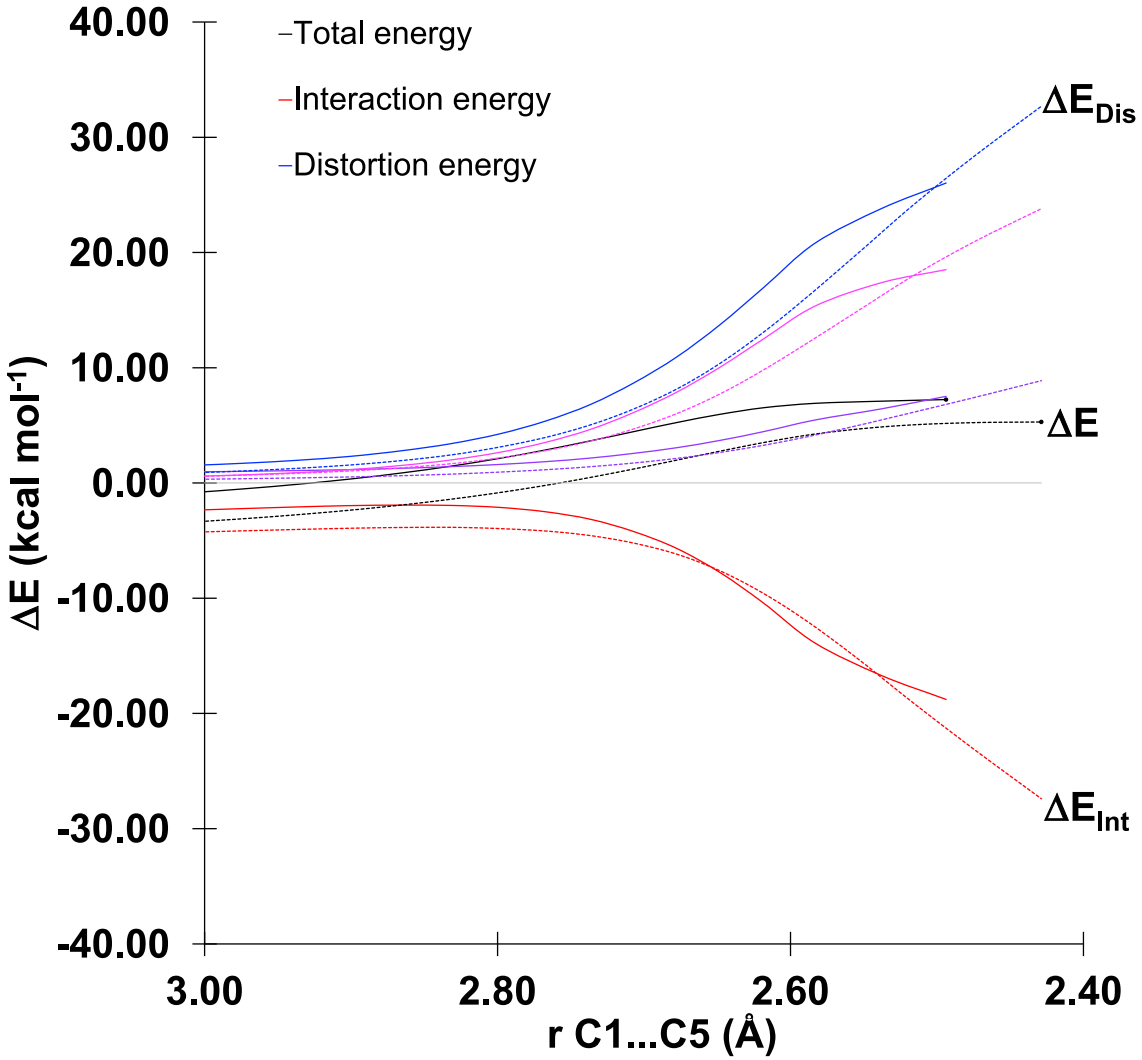

Fig. S2 Comparative DIAS diagrams for the **TS-on** (solid lines) and **TS-ox** (dashed lines) approaches of the 32CA reaction between **1** and **2** along the reaction coordinate projected onto the forming C1···C5 (right) bond distances. The transition states are indicated by a dot.

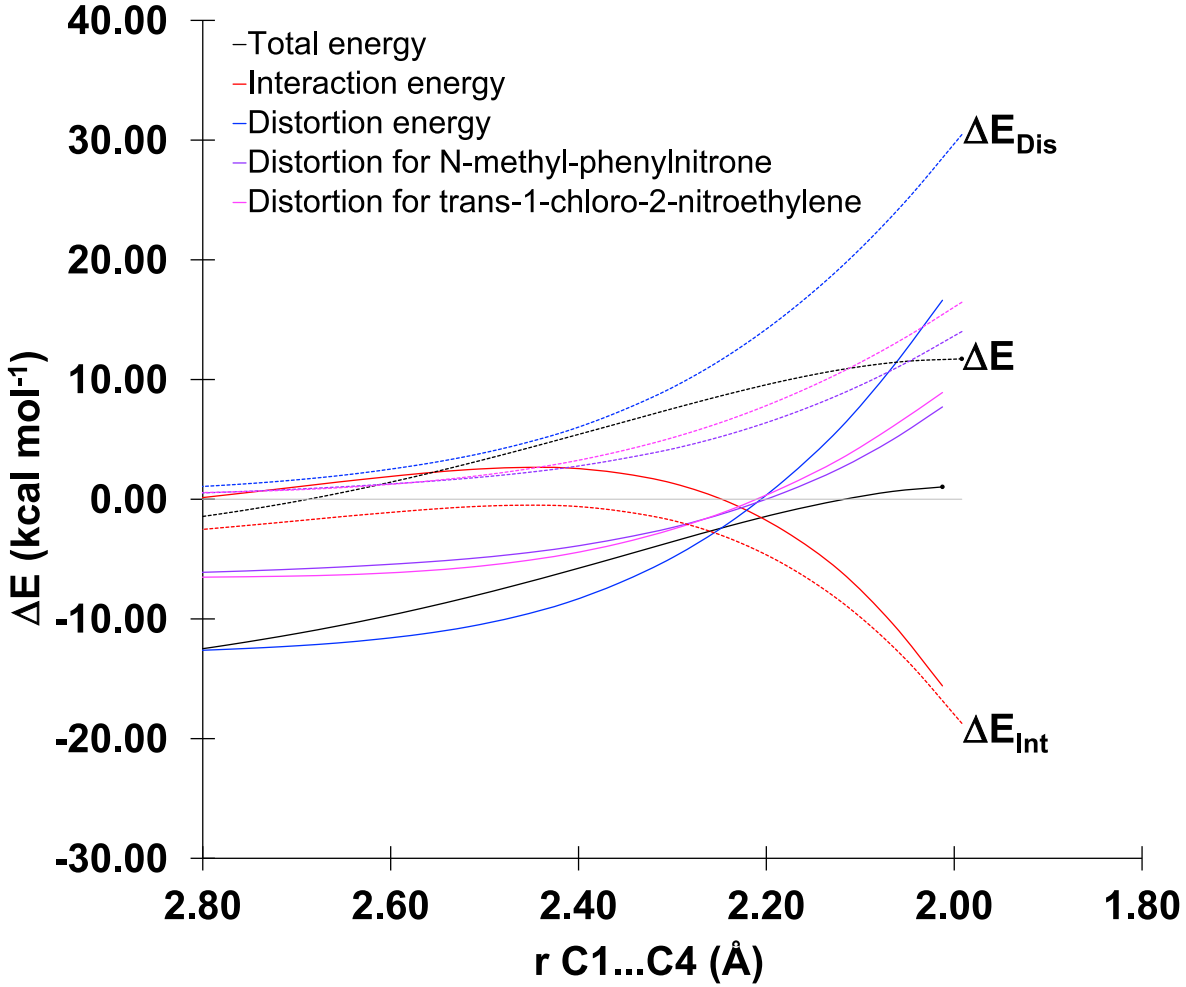

Fig. S3 Comparative DIAS diagrams for the **TS-mn** (solid lines) and **TS-mx** (dashed lines) approaches of the 32CA reaction between **1** and **2** along the reaction coordinate projected onto the forming and C1···C4 bond distances. The transition states are indicated by a dot.

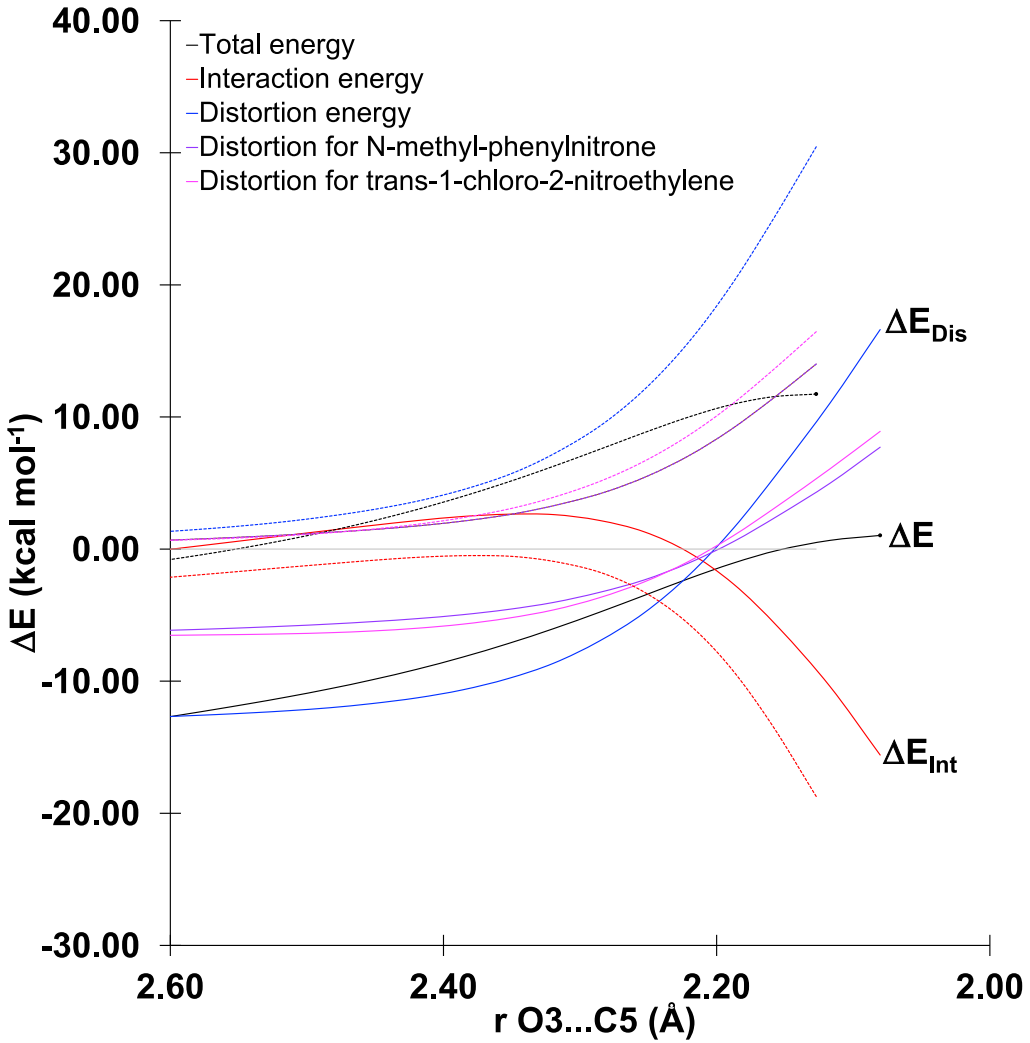

Fig. S4 Comparative DIAS diagrams for the **TS-mn** (solid lines) and **TS-mx** (dashed lines) approaches of the 32CA reaction between **1** and **2** along the reaction coordinate projected onto the forming O3···C5 bond distances. The transition states are indicated by a dot.

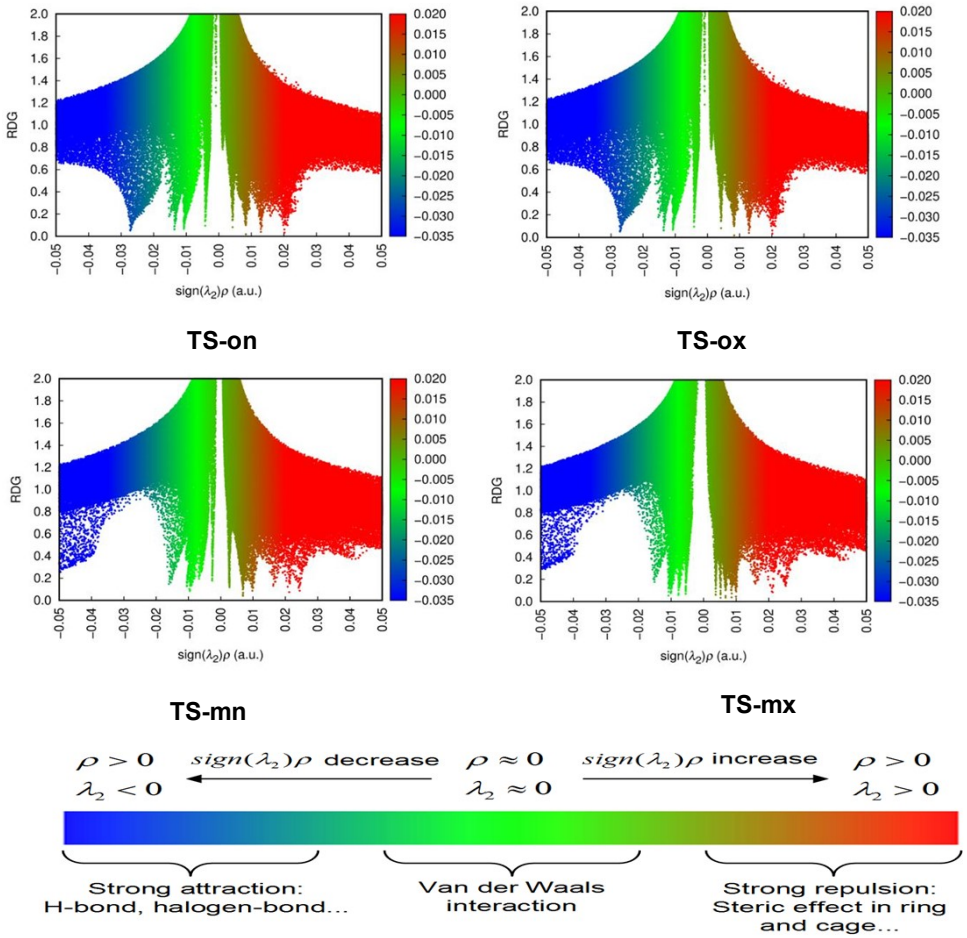

Fig. S5 The reduced density gradient and gradient isosurfaces of the TSs involved in the 32CA reaction between N-methyl-phenylnitrone **1** and trans-1-chloro-2-nitroethylene **2**.

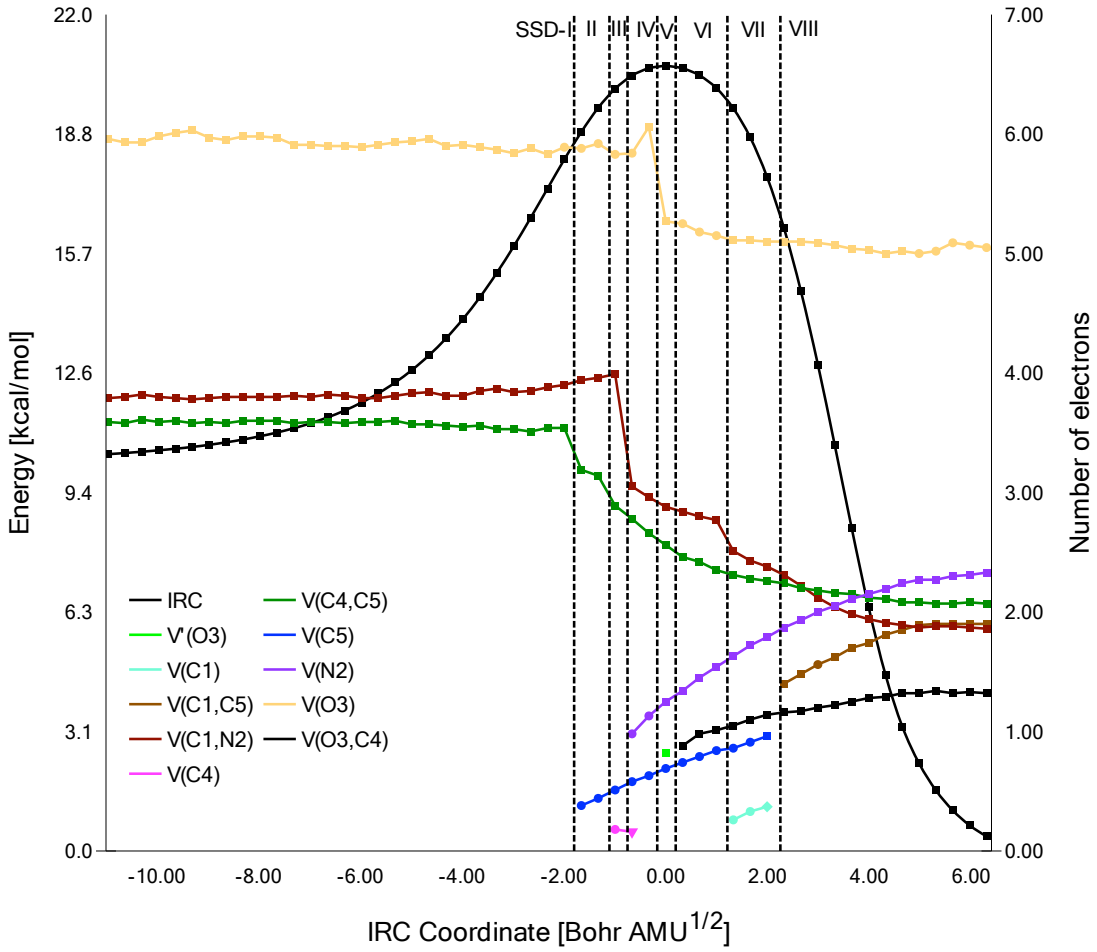

Fig. S6 Electron populations (e) evolution for selected basins along the IRC associated with the **TS-ox** regio-isomeric channel as determined at the IEFPCM(benzene)/B3LYP/6-311G(d,p) level of approximation. These evolutions are plotted on top of the potential energy surface.

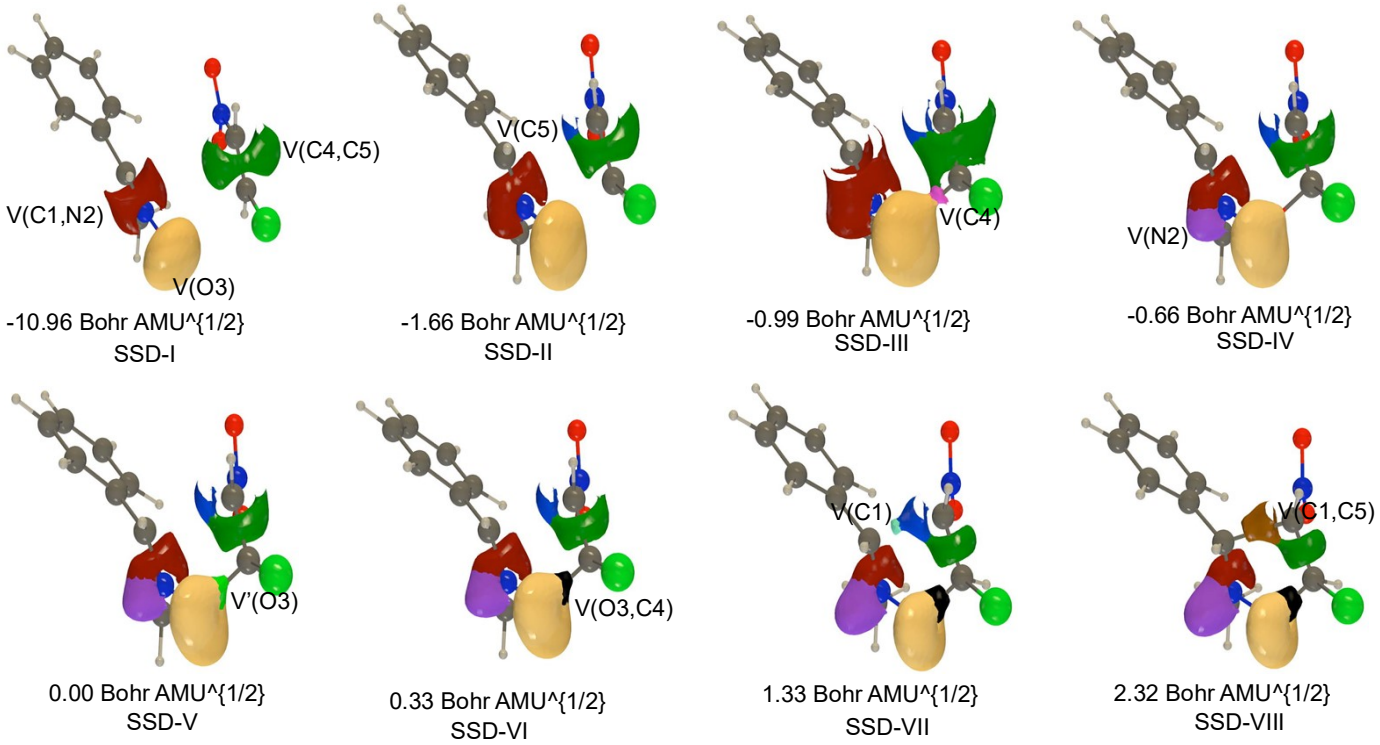

Fig. S7 ELF basin isosurfaces (η = 0.70) of each of the SSDs found along the IRC associated with **TS-ox**. Color labeling of the basins is adopted according to **Fig. S6**.

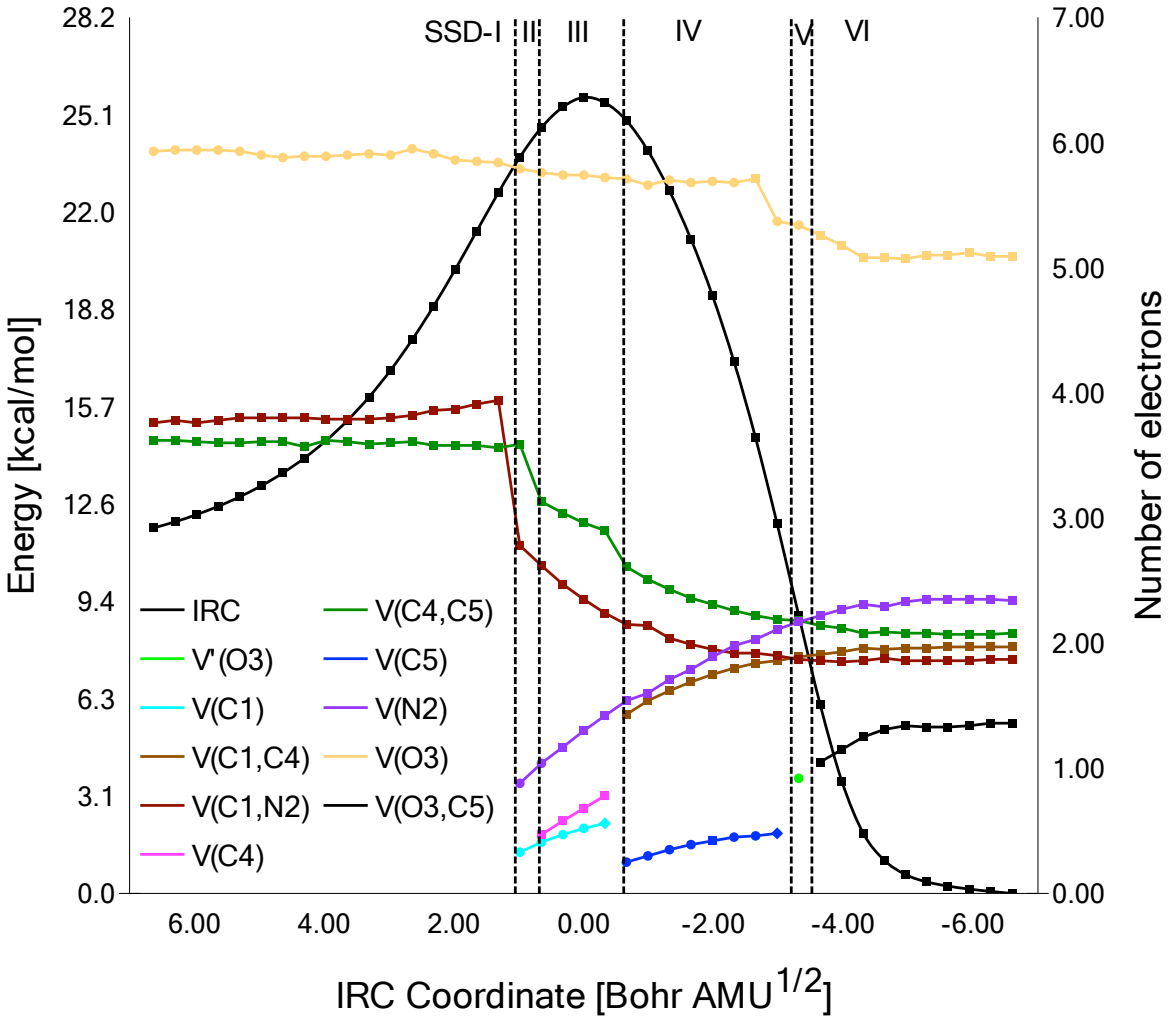

Fig. S8 Electron populations (e) evolution for selected basins along the IRC associated with the **TS-mn** regio-isomeric channel as determined at the IEFPCM(benzene)/B3LYP/6-311G(d,p) level of approximation. These evolutions are plotted on top of the potential energy surface.

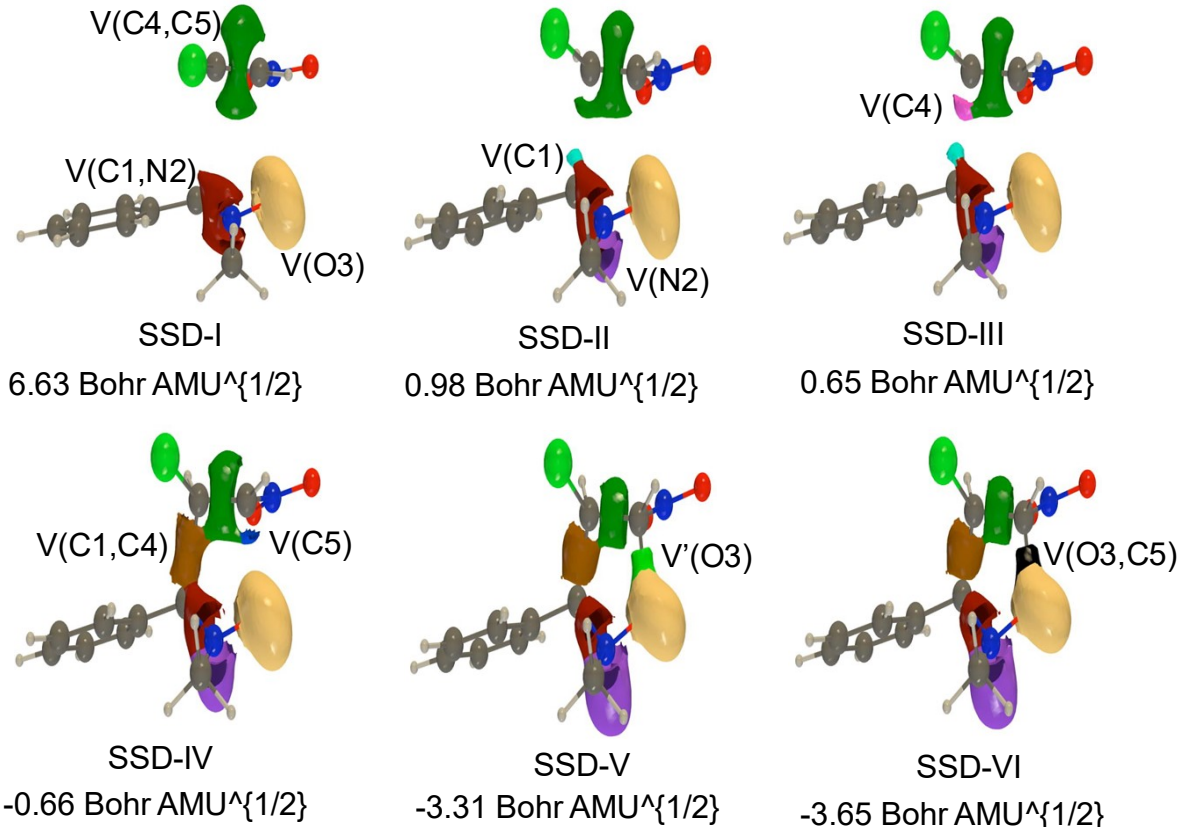

Fig. S9 ELF basin isosurfaces (η = 0.70) of each of the SSDs found along the IRC associated with **TS-mn**. Color labeling of the basins is adopted according to **Fig. S8**.

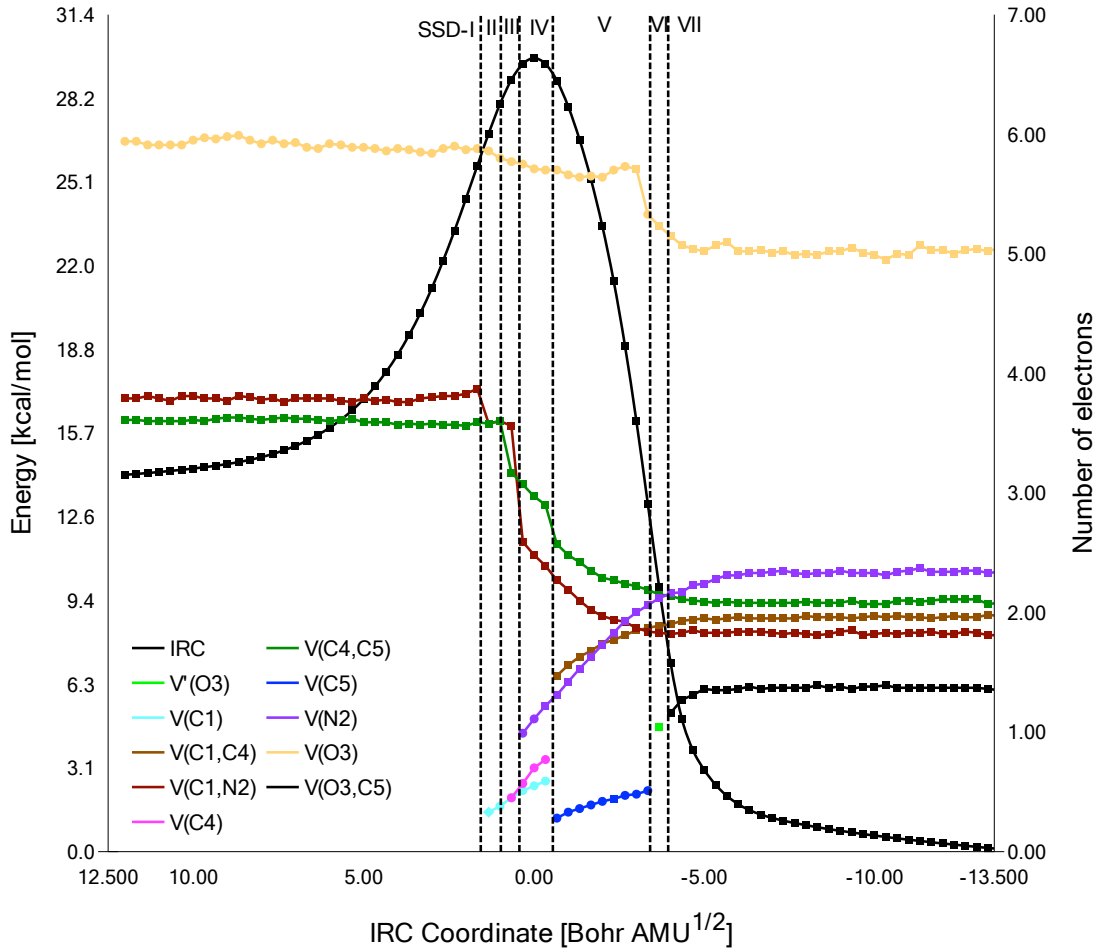

Fig. S10 Electron populations (e) evolution for selected basins along the IRC associated with the **TS-mx** regio-isomeric channel as determined at the IEFPCM(benzene)/B3LYP/6-311G(d,p) level of approximation. These evolutions are plotted on top of the potential energy surface.

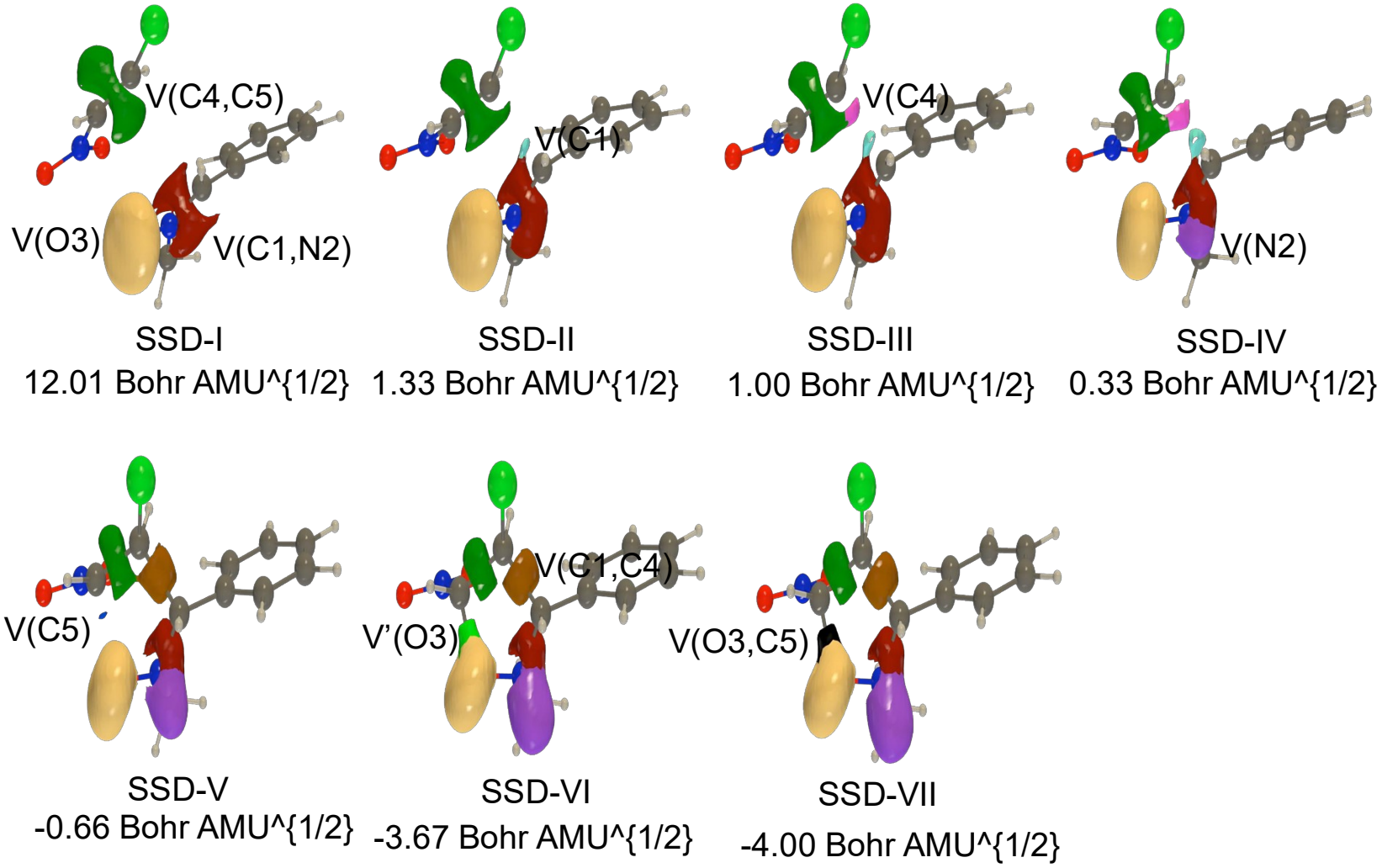

Fig. S11 ELF basin isosurfaces (η = 0.70) of each of the SSDs found along the IRC associated with **TS-mx**. Color labeling of the basins is adopted according to **Fig. S10**.

Table S7 Basin populations (in e), IRC coordinates (RX, Bohr $AMU^{1/2}$), relative electronic energies (ΔE in kcal/mol) and C1-C5/O3-C4 bond lengths (in Å) along the **TS-on** regio-isomeric channel of 32CA reaction.

	SSD-I		**SSD-II**		**SSD-III**		**SSD-IV**		**SSD-V**		**SSD-VI**		**SSD-VII**	
Basins	First	Last	First	Last	First	Last	First	Last	First	Last	First	Last	First	Last
V(C1,N2)	3.76	3.95	3.97	3.97	3.08	2.90	2.84	2.84	2.80	2.57	2.42	2.29	2.22	1.86
V(C4,C5)	3.60	3.59	3.20	3.20	2.94	2.76	2.65	2.65	2.53	2.30	2.29	2.25	2.21	2.09
V(O3)	5.99	5.84	5.88	5.88	5.85	5.92	5.42	5.42	5.23	5.10	5.09	5.02	5.04	4.96
V(N2)	---	---	---	---	0.94	1.20	1.30	1.30	1.40	1.67	1.75	1.90	1.97	2.30
V(C1)	---	---	---	---	---	---	---	---	---	---	0.21	0.34	---	---
V(C4)	---	---	---	---	0.19	0.19	---	---	---	---	---	---	---	---
V(C1,C5)	---	---	---	---	---	---	---	---	---	---	---	---	1.39	1.88
V(C5)	---	---	0.42	0.42	0.49	0.60	0.63	0.63	0.69	0.84	0.87	0.95	---	---
V'(O3)	---	---	---	---	---	---	0.73	0.73	---	---	---	---	---	---
V(O3,C4)	---	---	---	---	---	---	---	---	0.90	1.14	1.19	1.23	1.26	1.41
d(C1,C5)	3.177	2.648	2.618	2.618	2.583	2.494	2.472	2.472	2.453	2.294	2.233	2.107	2.043	1.532
d(O3,C4)	2.643	1.913	1.852	1.852	1.794	1.732	1.670	1.670	1.606	1.502	1.487	1.463	1.452	1.390
RX	6.89	1.29	0.95	0.95	0.59	0.00	-0.34	-0.34	-0.68	-1.72	-2.07	-2.77	-3.12	-6.97
E	13.46	21.35	21.93	21.93	22.31	22.64	22.35	22.35	21.96	20.61	19.94	17.89	16.44	0.00

Table S8 Basin populations (in e), IRC coordinates (RX, Bohr $AMU^{1/2}$), relative electronic energies (ΔE in kcal/mol) and C1-C5/O3-C4 bond lengths (in Å) along the **TS-ox** regio-isomeric channel of 32CA reaction.

	SSD-I		**SSD-II**		**SSD-III**		**SSD-IV**		**SSD-V**		**SSD-VI**		**SSD-VII**		**SSD-VIII**	
Basins	First	Last	First	Last	First	Last	First	Last	First	Last	First	Last	First	Last	First	Last
V(C1,N2)	3.79	3.90	3.94	3.96	3.99	3.99	3.05	2.96	2.88	2.88	2.84	2.77	2.51	2.38	2.31	1.86
V(C4,C5)	3.59	3.54	3.19	3.14	2.89	2.89	2.78	2.66	2.56	2.56	2.46	2.35	2.31	2.26	2.24	2.07
V(O3)	5.96	5.89	5.88	5.92	5.83	5.83	5.84	6.06	5.27	5.27	5.25	5.15	5.11	5.10	5.10	5.05
V(N2)	---	---	---	---	---	---	0.92	1.13	1.25	1.25	1.34	1.54	1.63	1.79	1.87	2.33
V(C1)	---	---	---	---	---	---	---	---	---	---	---	---	0.26	0.37	---	---
V(C4)	---	---	---	---	0.18	0.18	0.16	0.16	---	---	---	---	---	---	---	---
V(C1,C5)	---	---	---	---	---	---	1.39	1.88	1.39	1.39	---	---	---	---	1.39	1.88
V(C5)	---	---	0.38	0.44	0.51	0.51	0.58	0.63	0.69	0.69	0.74	0.84	0.86	0.96	---	---
V'(O3)	---	---	---	---	---	---	---	---	0.82	0.82	---	---	---	---	---	---
V(O3,C4)	---	---	---	---	---	---	---	---	---	---	0.88	1.01	1.05	1.14	1.16	1.32
d(C1,C5)	3.421	2.645	2.616	2.586	2.553	2.553	2.517	2.475	2.429	2.429	2.376	2.264	2.204	2.083	2.021	1.589
d(O3,C4)	2.748	1.954	1.897	1.841	1.796	1.796	1.753	1.696	1.644	1.644	1.611	1.561	1.542	1.510	1.496	1.413
RX	-10.96	-1.99	-1.66	-1.33	-0.99	-0.99	-0.66	-0.33	0.00	0.00	0.33	-0.99	1.33	1.99	2.32	6.96
E	10.42	18.16	18.88	19.51	20.01	20.01	20.36	20.55	20.61	20.61	20.55	20.03	19.50	17.69	16.35	0.00

Table S9 Basin populations (in e), IRC coordinates (RX, Bohr $AMU^{1/2}$), relative electronic energies (ΔE in kcal/mol) and C1-C4/O3-C5 bond lengths (in Å) along the **TS-mn** regio-isomeric channel of 32CA reaction.

	SSD-I		**SSD-II**		**SSD-III**		**SSD-IV**		**SSD-V**		**SSD-VI**	
Basins	First	Last	First	Last	First	Last	First	Last	First	Last	First	Last
V(C1,N2)	3.76	3.94	2.87	2.87	2.62	2.24	2.15	1.90	1.87	1.87	1.86	1.87
V(C4,C5)	3.62	3.56	3.59	3.59	3.13	2.90	2.61	2.19	2.18	2.18	2.14	2.08
V(O3)	5.93	5.84	5.79	5.79	5.76	5.72	5.71	5.37	5.34	5.34	5.26	5.09
V(N2)	---	---	0.88	0.88	1.04	1.42	1.54	2.11	2.17	2.17	2.22	2.34
V(C1)	---	---	0.33	0.33	0.41	0.56	---	---	---	---	---	---
V(C4)	---	---	---	---	0.47	0.78	---	---	---	---	---	---
V(C1,C4)	---	---	---	---	---	---	1.43	1.86	1.89	1.89	1.91	1.97
V(C5)	---	---	---	---	---	---	0.25	0.48	---	---	---	---
V'(O3)	---	---	---	---	---	---	---	---	0.92	0.92	---	---
V(O3,C5)	---	---	---	---	---	---	---	---	---	---	1.05	1.36
d(C1,C4)	2.915	2.240	2.181	2.181	2.122	1.953	1.890	1.630	1.614	1.614	1.599	1.548
d(O3,C5)	2.659	2.221	2.188	2.188	2.154	2.053	2.027	1.677	1.617	1.617	1.557	1.402
RX	6.36	1.32	0.99	0.99	0.65	-0.33	-0.66	-2.98	-3.31	-3.31	-3.64	-6.60
E	11.78	22.58	23.73	23.73	24.69	25.49	24.91	11.91	8.96	8.96	6.08	0.00

Table S10 Basin populations (in e), IRC coordinates (RX, Bohr $AMU^{1/2}$), relative electronic energies (ΔE in kcal/mol) and C1-C4/O3-C5 bond lengths (in Å) along the **TS-mx** regio-isomeric channel of 32CA reaction.

	SSD-I		**SSD-II**		**SSD-III**		**SSD-IV**		**SSD-V**		**SSD-VI**		**SSD-VII**	
Basins	First	Last	First	Last	First	Last	First	Last	First	Last	First	Last	First	Last
V(C1,N2)	3.79	3.87	3.58	3.58	3.60	3.56	2.59	2.39	2.27	1.84	1.83	1.83	1.82	1.81
V(C4,C5)	3.61	3.59	3.58	3.58	3.60	3.17	3.07	2.90	2.57	2.19	2.15	2.15	2.14	2.07
V(O3)	5.94	5.88	5.86	5.86	5.80	5.77	5.75	5.70	5.70	5.71	5.23	5.23	5.15	5.02
V(N2)	---	---	---	---	---	---	0.99	1.22	1.31	2.06	2.12	2.12	2.16	2.33
V(C1)	---	---	0.33	0.38	0.45	0.45	0.51	0.59	---	---	---	---	---	---
V(C4)	---	---	---	---	0.45	0.45	0.57	0.77	---	---	---	---	---	---
V(C1,C4)	---	---	---	---	---	---	---	---	1.47	1.87	1.89	1.89	1.90	1.98
V(C5)	---	---	---	---	---	---	---	---	0.28	0.51	---	---	---	---
V'(O3)	---	---	---	---	---	---	---	---	---	---	1.04	1.04	---	---
V(O3,C5)	---	---	---	---	---	---	---	---	---	---	---	---	1.16	1.36
d(C1,C4)	3.211	2.294	2.235	2.235	2.174	2.113	2.052	1.932	1.875	1.622	1.668	1.594	1.578	1.545
d(O3,C4)	2.877	2.282	2.250	2.250	2.220	2.190	2.159	2.095	2.058	1.627	1.566	1.566	1.566	1.401
RX	12.01	1.67	1.33	1.33	1.00	0.67	0.33	-0.33	-0.66	-3.33	-3.67	-4.00	-4.00	-13.32
E	14.12	25.70	26.92	26.92	28.03	28.93	29.53	29.53	28.90	13.04	9.90	7.08	7.03	0.00

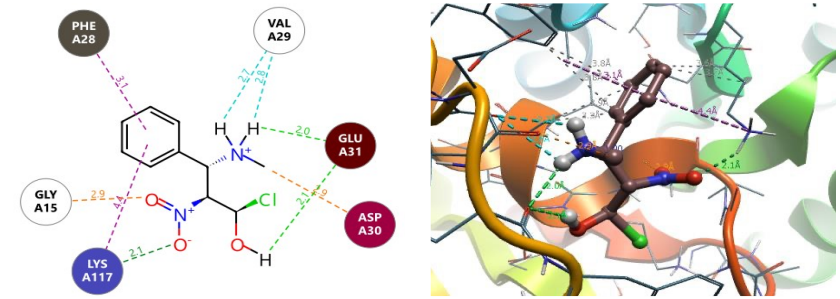

CA-mn

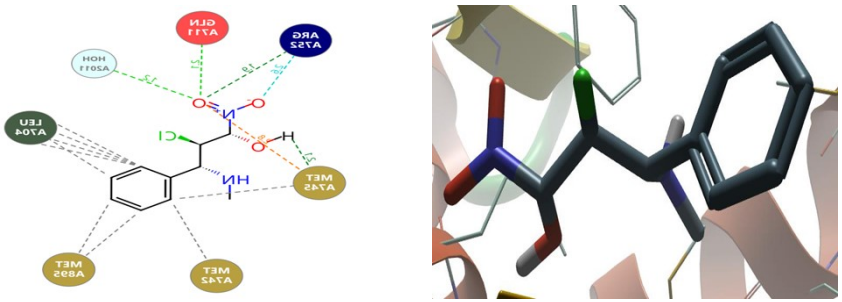

CA-mx

Fig. S12 2D and 3D visualization of the superimposed docking pose representation of binding interactions of **CA-mn**, and **CA-mx** compounds against HCT-116 (PDB ID: 4DSN).

Table S11 Binding affinity (kcal mol^{-1}) and nonbonding interactions of HCT-116 and compounds (**CA-ox**, **CA-on**, **CA-mn** and **CA-mx**).

Complex	Binding affinity (kcal mol^{-1})	Amino acid	Bond Type	Interaction	Distance (A˚)
Co-crystallized ligand	-13.095				
CA-ox		PHE28	Hydrophobic	Pi-Pi T-shaped	4.98628
		ALA146	Hydrophobic	Pi-Alkyl	5.11269
		ALA18	Hydrophobic	Pi-Alkyl	4.54263
		VAL29	Hydrogen Bond	Conventional Hydrogen Bond	2.69587
		VAL29	Hydrogen Bond	Conventional Hydrogen Bond	2.84979
		GLU31	Hydrogen Bond	Conventional Hydrogen Bond	2.14789
		GLU31	Hydrogen Bond	Conventional Hydrogen Bond	2.02953
		GLY15	Hydrogen Bond	Carbon Hydrogen Bond	2.29161
		ASN116	Hydrogen Bond	Carbon Hydrogen Bond	2.46196
		ASN116	Hydrogen Bond	Carbon Hydrogen Bond	2.68824
CA-on	-10.606	TYR32	Hydrophobic	Pi-Pi T-shaped	5.24707
		ALA18	Hydrophobic	Pi-Alkyl	4.83626
		THR35	Hydrogen Bond	Carbon Hydrogen Bond	3.09283
		GLY31	Hydrogen Bond	Conventional Hydrogen Bond	2.02026
		SER17	Hydrogen Bond	Carbon Hydrogen Bond	2.42552
		MG202	Electrostatic	Attractive Charge	2.34779
		ASP33	Hydrogen Bond	Carbon Hydrogen Bond	2.7383

CA-mn	ALA18	Hydrophobic	Pi-Alkyl	4.85427
	GLUA62	Hydrogen Bond	Conventional Hydrogen Bond	2.52329
	ASPA33	Hydrogen Bond	Carbon Hydrogen Bond	2.39761
	SERA17	Hydrogen Bond	Conventional Hydrogen Bond	1.82727
	SERA17	Hydrogen Bond	Carbon Hydrogen Bond	2.93186
	MG202	Electrostatic	Attractive Charge	3.81783
	LYSA16	Electrostatic	Attractive Charge	1.93392
	LYSA16	Hydrogen Bond	Conventional Hydrogen Bond	2.75855
	LYSA16	Hydrogen Bond	Conventional Hydrogen Bond	2.08189
	VALA14	Hydrogen Bond	Conventional Hydrogen Bond	2.77277
	GLYA13	Hydrogen Bond	Conventional Hydrogen Bond	2.1198
	GLY A15	Hydrogen Bond	Conventional Hydrogen Bond	2.04789
	GLN A99	Hydrophobic	Pi-Alkyl	5.19839
CA-mx	GLYA13	Halogen	Halogen (Cl, Br, I)	3.35043
	GLUA31	Hydrogen Bond	Conventional Hydrogen Bond	2.02111
	MG202	Electrostatic	Attractive Charge	2.47918
	MG202	Other	Metal-Acceptor	2.56646
	ASPA33	Hydrogen Bond	Conventional Hydrogen Bond	2.48819
	LYSA16	Electrostatic	Attractive Charge	4.21553
	LYSA16	Hydrogen Bond	Conventional Hydrogen Bond	2.95919
	SERA17	Hydrogen Bond	Conventional Hydrogen Bond	1.96692
	SERA17	Hydrogen Bond	Carbon Hydrogen Bond	2.81159
	SERA17	Hydrogen Bond	Carbon Hydrogen Bond	2.84992

H = Conventional hydrogen bond; C = Carbon hydrogen bond; A= Alkyl; PA = Pi-alkyl; PCa = Pi-cation; PS = Pi-sigma; PPT = Pi-Pi T-shaped; PDH = Pi-donor hydrogen bond; APS = Amide Pi-stacked.

Table S12 Drug-likeness predictions of compounds (**CA-ox**, **CA-on**, **CA-mn** and **CA-mx**), computed by SwissADME.

Compounds	Mol. Wt. (g/mol)	NHD	NHA	NRB	TPSA (A˚2)	Log P (iLOGP) lipophilicity	Log S (ESOL) water solubility	Synthetic accessibility	Lipinski's rule of five with zero violations
CA-on	242.66	0	4	2	58.29	1.90	-2.88	3.61	0
CA-ox	242.66	0	4	2	58.29	1.90	-2.88	3.61	0
CA-mn	242.66	0	4	2	58.29	1.69	-2.88	3.72	0
CA-mx	242.66	0	4	2	58.29	1.90	-2.88	3.72	0

Abbreviations: NHD, number of hydrogen donors; NHA, number of hydrogen acceptors; NRB, number of rotatable bonds; TPSA, total polar surface area.

Table S13 ADMET/pharmacokinetic features of the best-hit compounds.

Property	Value				Comment
	CA-on	**CA-mn**	**CA-ox**	**CA-mx**	Optimal: higher than -5.15 Log unit
Caco-2 Permeability	-4.742	-4.545	-4.688	-4.656	■ low permeability: < 2 × 10-6 cm/s ■ medium permeability: 2-20 × 10-6 cm/s ■ high passive permeability: > 20 × 10-6 cm/s
MDCK Permeability	-4.216	4.097	-4.223	-4.096	■ low permeability: < 2 × 10-6 cm/s ■ medium permeability: 2-20 × 10-6 cm/s ■ high passive permeability: > 20 × 10-6 cm/s
HIA	0.0	0.0	0.0	0.0	■ Human Intestinal Absorption ■ Category 1: HIA+(HIA < 30%); ■ Category 0: HIA-(HIA >= 30%); ■ The output value is the probability of being HIA+
F20%	0.001	0.003	0.004	0.003	■ 20% Bioavailability ■ Category 1: F 20% + (bioavailability < 20%); ■ Category 0: F 20% - (bioavailability ≥ 20%); ■ The output value is the probability of being F 20%
F30%	0.004	0.022	0.018	0.012	■ 30% Bioavailability ■ Category 1: F 30% + (bioavailability < 30%); ■ Category 0: F 30% - (bioavailability ≥ 30%); ■ The output value is the probability of being F 30% +

Table S14 ADME predictions of compounds (**CA-ox**, **CA-on**, **CA-mn** and **CA-mx**), computed by SwissADME and PreADMET.

S.No.	Formula	Skin Permeation value (log Kp) cm/s	GI absorption	BBB Permeability	Pgp substrate	Inhibitor Interaction (SwissADME/PreADMET)				
						CYP1A2 inhibitor	CYP2C19 inhibitor	CYP2C9 inhibitor	CYP2D6 inhibitor	CYP3A4 inhibitor
CA-ox	$C_{10}H_{11}ClN_2O_3$	-6.22	High	Yes	No	No	No	No	No	No
CA-on	$C_{10}H_{11}ClN_2O_3$	-6.22	High	Yes	No	No	No	No	No	No
CA-mn	$C_{10}H_{11}ClN_2O_3$	-6.22	High	Yes	No	No	No	No	No	No
CA-mx	$C_{10}H_{11}ClN_2O_3$	-6.22	High	Yes	No	No	No	No	No	No

Abbreviations: Log Kp, skin permeation value; GI, gastro-intestinal; BBB, blood-brain barrier; P-gp, P-glycoprotein; CYP, cytochrome-P.

Table S15 Prediction of toxicity of compounds (**CA-ox**, **CA-on**, **CA-mn** and **CA-mx**), computed by Pro-Tox II and OSIRIS property explorer

S.No.	Formula	LD_{50} (mg/kg)	Toxicity class	Organ Toxicity					
				Hepatotoxicity	Carcinogenicity	Immunotoxicity	Mutagenicity	Cytotoxicity	Irritant
CA-ox	$C_{10}H_{11}ClN_2O_3$	1000	4	Active	Active	Inactive	Active	Inactive	No
CA-on	$C_{10}H_{11}ClN_2O_3$	1000	4	Active	Active	Inactive	Active	Inactive	No
CA-mn	$C_{10}H_{11}ClN_2O_3$	1000	4	Active	Active	Inactive	Active	Inactive	No
CA-mx	$C_{10}H_{11}ClN_2O_3$	1000	4	Active	Active	Inactive	Active	Inactive	No